lubricants

MDPI

Communication

Catalytic and Tribological Performances of a Novel Bi-Functional Ionic Liquid in Lubricating Ester Oil

Yanan Wang [1,2], Huaigang Su [1,2], Jun Yin [1,2], Cheng Jiang [1,2], Qilong Zhao [1,2], Wenjing Lou [1,2,*] and Qian Jia [1,2]

[1] State Key Laboratory of Solid Lubrication, Lanzhou Institute of Chemical Physics, Chinese Academy of Sciences, No. 18 Tianshui Middle Road, Lanzhou 730000, China; ynwang@licp.cas.cn (Y.W.); suhg@licp.cas.cn (H.S.); yinjun@licp.cas.cn (J.Y.); jiangcheng@licp.cas.cn (C.J.); zhaoqilong@licp.cas.cn (Q.Z.); jiaqian@licp.cas.cn (Q.J.)

[2] Qingdao Key Laboratory of Lubrication Technology for Advanced Equipment, Qingdao Center of Resource Chemistry & New Materials, Qingdao 266100, China

* Correspondence: wjlou@licp.cas.cn; Tel.: +86-0532-58561709

Abstract: To address the detrimental effects of the residue of catalysts on the tribological performances of ester lubricants, a novel and efficient bi-functional ionic liquid 1-(3,5-di-tert-butyl-4-hydroxybenzyl)-3-methylimidazole di(2-ethylhexyl) phosphate ([(BHT-1)MIM][DEHP]) was prepared. The catalyst not only facilitates the synthesis of pentaerythritol tetra-hexanoate (PETH) through the catalytic esterification reaction—achieving up to 96% conversion with a 94% yield—but also enhances the tribological performance of ester oil PETH when used as a lubricant additive. The tribological property has been improved remarkably: the mean friction coefficient for PETH + [(BHT-1)MIM][DEHP] is notably lower, at 0.110, compared to the PETH, which has a coefficient of 0.180. Meanwhile, the wear scar diameter of the steel ball, when lubricated with PETH + [(BHT-1)MIM][DEHP], is notably smaller than that of a steel ball lubricated solely with PETH. Especially, the reduction in the wear volume at 100 °C is up to 81.46% compared with the base oil PETH. [(BHT-1)MIM][DEHP], PETH + [(BHT-1)MIM][DEHP], and the worn track of the upper running ball and lower disc were systematically characterized by using Nuclear Magnetic Resonance (NMR) spectra, a Fourier Transform Infrared Spectrometer (FT-IR), a field emission scanning electron microscope (FESEM), Thermal gravity analysis (TG), X-ray photoelectron spectroscopy (XPS), and an optical microscope (OM). The wear mechanism of the tailored lubricant oil was discussed in terms of the chemical composition of the worn surface.

Keywords: bi-functional ionic liquid; ester oil; catalyst; lubricant additive

check for updates

Received: 1 November 2024
Revised: 9 January 2025
Accepted: 20 January 2025
Published: 22 January 2025

Citation: Wang, Y.; Su, H.; Yin, J.; Jiang, C.; Zhao, Q.; Lou, W.; Jia, Q. Catalytic and Tribological Performances of a Novel Bi-Functional Ionic Liquid in Lubricating Ester Oil. *Lubricants* **2025**, *13*, 45. https://doi.org/10.3390/lubricants13020045

Copyright: © 2025 by the authors. Licensee MDPI, Basel, Switzerland. This article is an open access article distributed under the terms and conditions of the Creative Commons Attribution (CC BY) license (https://creativecommons.org/licenses/by/4.0/).

1. Introduction

With the advancement of modern science and technology, the high speed, heavy load, and high precision of machinery and equipment are developing increasingly, and the requirements for lubricating oil are becoming higher and higher. Thus, the research and application of polyol ester oil with excellent thermal and oxidation stability, good high- and low-temperature performance, and biodegradability and tribological performance improvement have received more and more attention [1–4]. Ester oil is the most widely used synthetic oil besides synthetic hydrocarbon oil. Among them, polyol ester oil has excellent comprehensive performance. Polyol ester is obtained by the esterification of polyols, including neopentyl glycol, pentaerythritol, and trimethylol propane with long-chain carboxylic acid (generally C_8~C_{12} or oleic acid). They have good heat and oxidation

resistance, lubricity, viscosity temperature, and evaporation performance. In addition, the lubrication performance of polyol ester is better than that of diester and mineral oil and is far better than that of polyalphaolefin (PAO). Notably, the long- and short-chain mixed ester has the lower friction coefficient [5].

Alkaline and acid could be used for the synthesis of polyol ester; however, the alkaline catalyst is sensitive to fatty acid and H_2O in the base oil, where the hydrolysis and saponification might be induced [6]. Therefore, the polyol ester lubricating oil is generally synthesized through esterification reactions with acid catalysts during industrial production, such as concentrated sulfuric acid, p-toluene sulfonic acid, etc., by traditional high-temperature heating methods [7,8]. Because the used catalysts also have the functions of oxidation, sulfonation, dehydration, and isomerization, a series of side reactions always occur. The reaction products and the follow-up treatment are complicated, and a large amount of waste liquid is produced, which pollutes the environment. At the same time, the concentrated sulfuric acid seriously corrodes the equipment. These directly lead to the synthesized polyol ester having a darker colour, displaying poor purity, and being unable to obtain high-quality products, which directly affect their application in some industries with high product quality requirements. People's awareness of environmental protection is increasing day by day, and the laws and the regulations of environmental protection are gradually improving. Figuring out new efficient and environmentally friendly catalysts to replace traditional concentrated sulfuric acid and developing new environmentally friendly synthesis methods have been the focus of esterification research. The research on the synthesis of polyol esters is mainly focused on the synthesis and selection of catalysts, including solid acid catalysts, ionic liquid catalysts, and enzyme catalysts [9–11]. Zirconium phenylphosphonate phosphite has been utilized as a highly effective, recyclable, solid acid catalyst for the synthesis of fatty acid polyol esters, and the catalyst demonstrates excellent catalytic efficiency, notably with a high selectivity of 92.3 mol% for (di + tri) esters [9]. Ma et al. [11] found that the R. glutinis lipid, characterized by its high oleic acid content, was esterified with trimethylolpropane (TMP) using the Candida enzyme in a solvent-free system, achieving a trimethylolpropane fatty acid triester (TFAT) yield of 89.5%. The synthesis methods include direct esterification and transesterification [5,12]. In the heating method, prior studies have disclosed the use of microwave radiation to replace the common heating method, having achieved good results. In order to protect the environment and the sustainable development of energy, it is necessary to study and develop the green synthesis of polyol esters.

Ionic liquid has demonstrated considerable catalytic effectiveness within the realm of organic synthesis and catalysis. Gupta et al. [13] prepared an innovative acetate-based butylimidazolium ionic liquid immobilized on silica-coated magnetic nanoparticles, serving as an environmentally friendly catalyst. This catalyst achieved over 99% conversion and selectivity for N-aryl oxazolidin-2-ones. A novel ionic liquid catalyst, proline trifluoromethanesulfonate, exhibited high catalytic efficiency in the esterification of oleic acid, achieving an oleic acid conversion rate of up to 98.97%. Additionally, a potential reaction mechanism for the [ProH][CF_3SO_3]-catalyzed esterification process was discussed [14]. Cai et al. [15] synthesized five novel amino-acid-functionalized ionic liquids using methanesulfonic acid and amino acids (AAs). The catalytic properties of the ionic liquids were assessed for biodiesel production through the reaction of oleic acid and methanol to form esters. Among the synthesized catalysts, IL [GluH][CH_3SO_3] demonstrated the highest catalytic efficiency in oleic acid esterification, achieving a conversion rate of 96.8%. Notably, the catalytic performance of [GluH][CH_3SO_3] remained stable over ten consecutive esterification cycles. In addition, another property of ionic liquids, lubrication performance, is concerned. As a lubricant, ionic liquid has a wide liquid temperature range and very low

vapour pressure so that it may have excellent comprehensive lubrication properties that are incomparable with other lubricating materials. For example, the ionic liquids can solve the problems of the solidification and volatile loss of lubricants under harsh conditions. Ionic liquids are expensive to use as pure lubricants compared to other synthetic hydrocarbon oils. Hence, the use of ionic liquid as an efficient additive for lubricating oil is an effective way with high cost performance and wide industrial application. Roy et al. [16] investigated the use of a phosphonium phosphate ionic liquid as an additive to enhance anti-wear and anti-pitting performance in rear axle lubricants. When incorporated into VHVI8 base oil at concentrations of 2–3%, the ionic liquid provided effective surface protection against wear and micro-cracking under rolling–sliding conditions. Experimental oils containing this additive outperformed a commercial SAE 75W-90 gear oil in mitigating rolling contact fatigue during bench-scale rolling–sliding tests. Bai et al. [17] prepared a series of protic ionic liquids based on 1,8-diazabicyclo[5.4.0]undecane-7-ene-organophosphoric acid through neutralization. These ionic liquids, featuring dianionic and dicationic structures within a single molecular, were evaluated as additives in PAO-10 lubricants. Their application resulted in a friction coefficient reduction of up to 60% and a wear volume decrease of 83%. Fang et al. [18] developed an oil-soluble IL lubricant additive, 2-N-undecylimidazolium bis(2-ethylhexyl) phosphate [C11-IM][DEHP], through a "bottom-up" structural design approach. Compared to the commercially additive zinc dialkyl dithiophosphates (ZDDPs) and other existing oil-soluble ILs, [C11-IM][DEHP] demonstrated markedly superior lubrication performance, even under high normal loads of 400 N. Notably, at a concentration tenfold lower than the conventional dosage, [C11-IM][DEHP] maintained a COF as low as 0.1 under extreme load conditions. Up to now, the catalyst still needs to be separated from the esterification system for the polyol ester oil synthesis after the reaction. Therefore, there is a desperate need to develop a new material which functions both as a catalyst and a lubricant additive.

This study presents a novel and efficient bi-functional ionic liquid, specifically 1-(3,5-di-tert-butyl-4-hydroxybenzyl)-3-methylimidazole di(2-ethylhexyl) phosphate, denoted as [(BHT-1)MIM][DEHP], was synthesized. It was employed not only as a catalyst in the esterification reaction for the production of lubricating ester oil, but also as an additive for the ester oil after esterification, without the necessity of separation. It exhibited excellent catalytic activity for the esterification of pentaerythritol with caproic acid under mild conditions; the esterification rate was up to 96% with a 94% yield. Notably, the ionic liquid did not require separation after the esterification. Subsequently, it served as a lubricant additive, markedly enhancing the tribological properties of the base oil pentaerythritol tetra-hexanoate.

2. Materials and Methods

2.1. Materials

All chemicals were obtained from commercial sources and used without additional purification. The purity and vendors are listed in Table S1 in Supplementary Material.

HDN-26 was purchased from NanDa Synthetic Chemical Co., Ltd. (Jiangyin, China).

2.2. The Preparation of the Bi-Functional Ionic Liquid [(BHT-1)MIM][DEHP]

Step 1:

A mixture of 2,6-Di-tert-butyl-4-methylphenol (90.29 mmol), N-Bromosuccinimide (NBS: 436.08 mmol), and 2,2′-Azobis(2-methylpropionitrile) (AIBN: 39.03 mmol) in trichloromethane ($CHCl_3$: 860 mL) was stirred for 10 h under N_2 atmosphere at 65 °C after degassing. After the reaction, the products were filtered, and the filtrate was concentrated

using rotary evaporation, yielding 2,6-di-tert-butyl-4-bromomethylphenol (121 g) as a white solid (Figure 1).

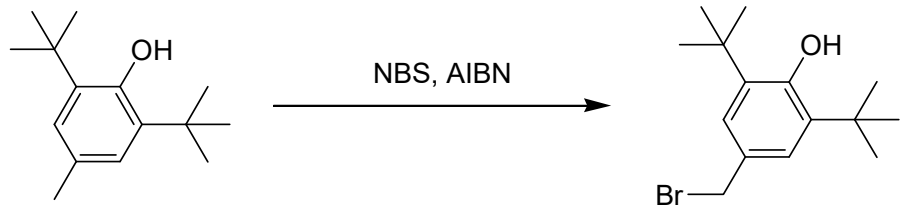


Figure 1. The scheme for the synthesis of 2,6-di-tert-butyl-4-bromomethylphenol.

Step 2:

1-methylimidazole (200.50 mmol) was added to a solution of 2,6-di-tert-butyl-4-bromomethylphenol (200.50 mmol) dissolved in acetonitrile (ACN: 1500 mL), and the mixture was stirred at 25 °C for 6 h. Upon completion, the products were mixed with methyl tert-butyl ether (MTBE: 3000 mL) at 25 °C, and the filtrate was dried in a vacuum oven to obtain 1-(3,5-di-tert-butyl-4-hydroxybenzyl)-3-methyl imidazole bromide (61.5 g) as a white solid (Figure 2).

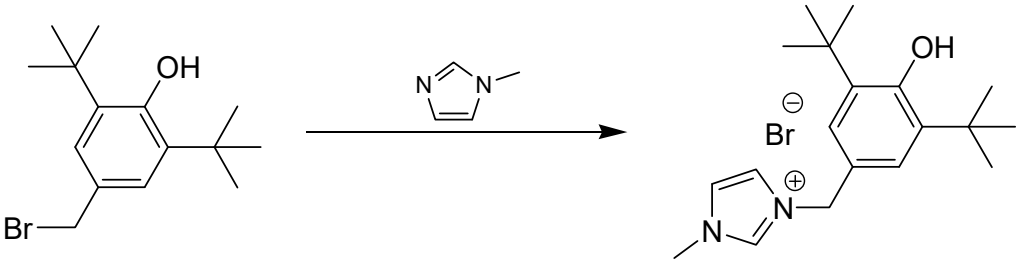


Figure 2. The scheme for the synthesis of 1-(3,5-di-tert-butyl-4-hydroxybenzyl)-3-methyl imidazole bromide.

Step 3:

Bis(2-ethylhexyl) hydrogen phosphate (37.66 mmol) was added into potassium hydroxide solution (37.66 mmol KOH in 50 mL H_2O) and stirred for 2 h at 25 °C. Then, a solution of dichloromethane (DCM: 150 mL), which contained 1-(3,5-di-tert-butyl-4-hydroxybenzyl)-3-methyl imidazole bromide (37.66 mmol), was poured into the above solution and then stirred for 12 h. After the reaction, the product was extracted 3 times with DCM. The mixed organic layers were dried in a vacuum oven to achieve the crude product, and the crude product was triturated with MTBE and 2-isopropoxypropane for 1 h, respectively. 1-(3,5-di-tert-butyl-4-hydroxybenzyl)-3-methylimidazole di(2-ethylhexyl) phosphate ([(BHT-1)MIM][DEHP]) was obtained as a yellow oil (Figure 3), and the structure was characterized by NMR, HPLC, HRMS, and CHNS-O element analysis. The purity of [(BHT-1)MIM][DEHP] was 96.17%, which was determined by the peak area ratio of [(BHT-1)MIM][DEHP] in all the peaks of the HPLC spectra. The spectra of HPLC and CHNS-O element analysis are provided in the Supplementary Material in Figure S1 and Table S2.

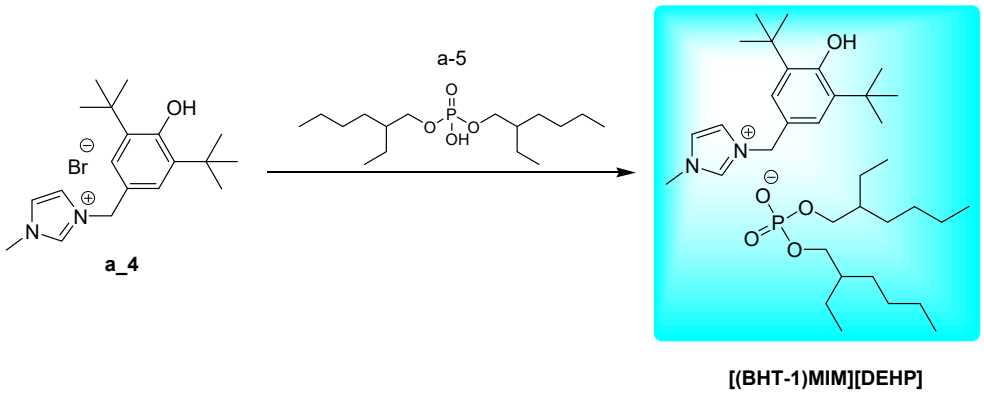


Figure 3. The scheme for the synthesis of 1-(3,5-di-tert-butyl-4-hydroxybenzyl)-3-methylimidazole di(2-ethylhexyl) phosphate.

2.3. The Catalytic Performance Test of [(BHT-1)MIM][DEHP]

Since PETH is a commonly used base oil in aviation engine oils and transformer oils, we chose the esterification reaction of pentaerythritol with caproic acid as a representative model to evaluate the catalytic performance of [(BHT-1)MIM][DEHP] (Figure 4); the specific experimental device is supplied in Figure S2 in the Supplementary Material. The reaction was carried out in a flask, where 0.013 mol pentaerythritol, 0.052 mol caproic acid, and the catalyst ([(BHT-1)MIM][DEHP] content: 0.8 g) were introduced. Then, 2 mL toluene was also added as a water-removing agent to react for a specified time at 160 °C. The product was evaporated by rotation. The acid value of the product was measured by reference [19], and the esterification rate of the product was analyzed by the acid value. The esterification rate could be calculated by the following formula:

$$\mathrm{Er}/\% = [(1 - \mathrm{AN_a}/\mathrm{AN_b}) \times \mathrm{R}/4] \times 100\%$$

where Er represents the conversion of caproic acid, $\mathrm{AN_a}$ is the acid number of products, and $\mathrm{AN_b}$ is the acid number of substrates. R represents the molar ration of caproic acid to pentaerythritol.

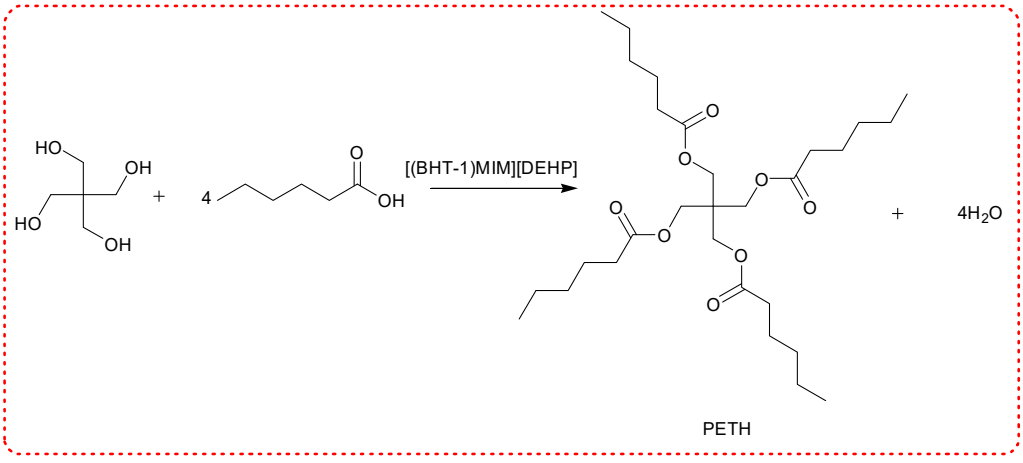


Figure 4. The catalytic reaction of pentaerythritol with caproic acid.

The yield of PETH was determined by quantitative ^{1}H NMR, with triphenylmethane as the internal standard of these products, and was calculated by the following formula:

1.

$$\mathrm{Yield}/\% = \frac{\mathrm{m}}{\mathrm{m_{weighting}}} \times 100\%$$

2. The m was calculated by the following formula:

$$\frac{\frac{m_{triphenylmethane}}{M_{triphenylmethane}}}{\frac{8m}{M_{pentaerythrotoltetra-hexanoate}}} = \frac{n_{1H}}{n_{8H}}$$

where m represents the weight of PETH in the products, $m_{weighing}$ represents the weight of products, $m_{triphenylmethane}$ represents the weight of triphenylmethane, $M_{triphenylmethane}$ represents the molecular weight of triphenylmethane, and $M_{pentaerythritoltetrahexanoate}$ represents the molecular weight of pentaerythritol tetra-hexanoate.

In order to provide further evidence on the characterization of the produced polyol ester, the ionic liquid [(BHT-1)MIM][DEHP] was separated from the products after the esterification reaction; the products were extracted 3 times with MTBE. The mixed organic layers were dried in a vacuum oven to obtain the polyol ester, and the structure was characterized by NMR.

2.4. Tribological Performance Test of [(BHT-1)MIM][DEHP]

The tribological performance test was assessed using an Optimol SRV tester under a 50 N load, 25 Hz frequency, 100 °C, 1 mm stroke, and 30 min duration in a ball-on-disc setup. The upper ball, made of AISI52100 steel, had a diameter of 10 mm, a rock-well hardness of 60 HRC, and a root-mean-square (RMS) roughness of 20 nm. The lower disc, also made of AISI52100 steel, had a diameter of 24 mm, a rock-well hardness of 60 HRC, and an RMS roughness of 20 nm. The friction coefficient was automatically monitored using a computer. Each experiment utilized 0.5 mL of lubricant, and tests were repeated three times to verify the consistency of the results.

2.5. Characterization

The kinematic viscosity of PETH and PETH + [(BHT-1)MIM][DEHP] was tested by SVM 3000 (Anton Paar), and the viscosity index was ascertained in accordance with ASTMD 2270-10, while the copper strip test was conducted following the protocol of ASTMD 130-10 (temperature: 100 °C, duration: 3 h).

Thermo-gravimetry (TG) was assessed by employing a Pyris Diamond TG/DTA analyzer at a heating rate of 10 °C/min under nitrogen atmosphere from 25 °C to 1000 °C. The X-ray photoelectron spectroscopy (XPS) analysis was conducted using a Thermo K-Alpha+ instrument with Al Kα radiation at 1486.8 eV. Fourier Transform Infrared Spectrometer (FT-IR) spectra were recorded on a Thermo Nicolet 5700 FT-IR spectrophotometer.

Nuclear Magnetic Resonance (NMR) spectra of ester was measured using a Bruker ARX 400 spectrometer at 400 MHz (^{1}H). The quantitative ^{1}H NMR was measured using a Bruker AVANCE III 600 spectrometer at 600 MHz (^{1}H): a pulse angle of 90°, a probe temperature of 25 °C, no spin, a scan number of 8, a spectral width of 20 ppm, an acquisition time of 1.363 s, a relaxation delay of 60 s, and a pulse width of 7.05 μs. All spectra were recorded in $CDCl_3$, and chemical shifts (δ) are reported in ppm relative to tetramethylsilane referenced to the residual solvent peaks.

High-Performance Liquid Chromatography (HPLC) chromatographic separations were performed on a HPLC system equipped with an Agela HP-Q-P050 pump and an Agela HP-Q-UV100Z detector (Agela Technologies, Tianjin, China). High-resolution mass spectrometry (HR-MS) was assessed using a time-of-flight detector (MAXIS ULTIMATE 3000 RSLCNANO-TOF-MS, Thermo Fisher Scientific, Waltham, MA, USA) working with a positive electrospray ion source (ESI+) and acquiring data in full-scan mode, from 50 to 1000 amu.

A field emission scanning electron microscope (FESEM) was used to scan the morphologies of worn tracks lubricated by PETH and PETH + [(BHT-1)MIM][DEHP]. The Optical microscope (OM) was used to measure the wear scar diameter of the upper running ball lubricated by PETH and PETH + [(BHT-1)MIM][DEHP].

3. Results

3.1. Structural Characterization and Stability Analysis of [(BHT-1)MIM][DEHP]

The structure of [(BHT-1)MIM][DEHP] was characterized by NMR and HRMS. The NMR spectra are provided in the Supplementary Material (Figures S3 and S4), and the NMR data are as follows:

^{1}H NMR: ($CDCl_3$, 400 MHz, TMS) δ = 10.90 (s, 1H), 7.14 (s, 2H), 7.07 (s, 1H), 6.93 (s, 1H), 5.43–5.33 (m, 3H), 4.09 (s, 3H), 3.78 (d, J = 5.8 Hz, 4H), 1.59–1.47 (m, 2H), 1.42 (s, 18H), 1.38–1.30 (m, 6H), 1.26 (d, J = 4.6 Hz, 10H), 0.82 (t, J = 7.4 Hz, 12H).

^{13}C NMR: ($CDCl_3$, 400 MHz, TMS) δ = 154,74, 138.93, 137.23, 125.99, 123.58, 123.11, 120.77, 67.72, 53.80, 40.32, 34.36, 30.16, 29.01, 23.32, 23.06, 14.07, 10.94.

The HR-MS is shown in Figure 5.

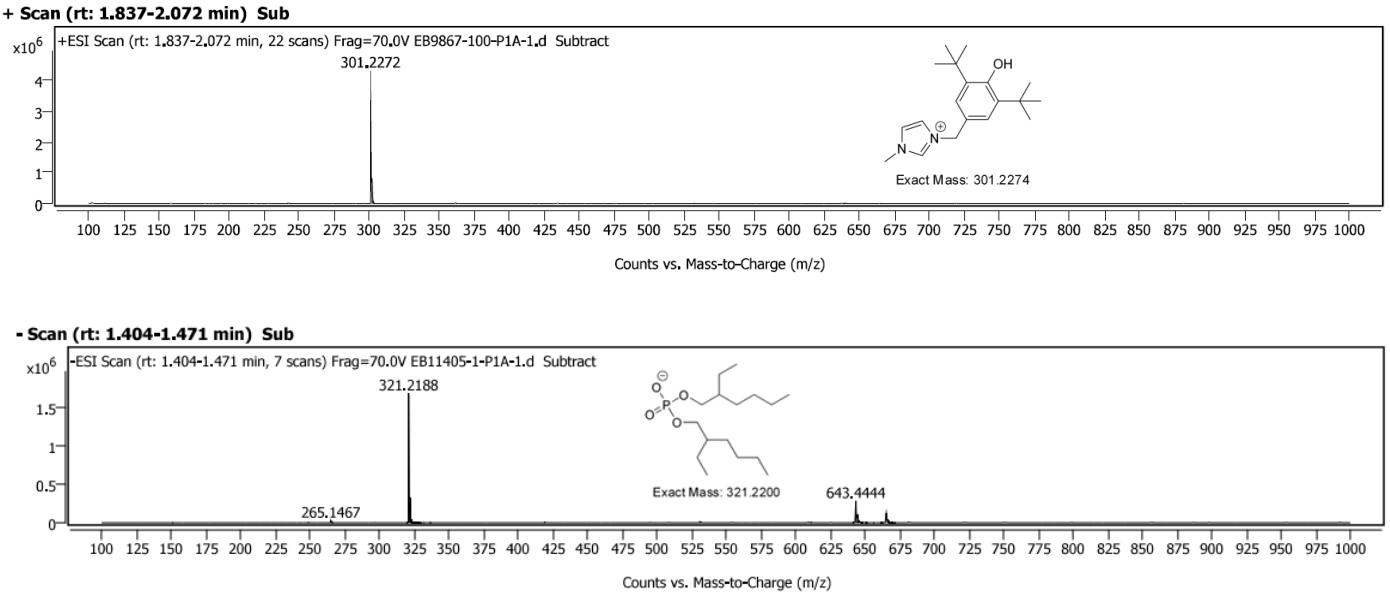


Figure 5. The HR-MS of [(BHT-1)MIM][DEHP].

According to the HR-MS spectra, we can determine the structure of the ionic liquid [(BHT-1)MIM][DEHP]. Meanwhile, the purity of [(BHT-1)MIM][DEHP] was verified by NMR, HPLC, and an Element analyzer. The results of THE element C, H, O, N contents of [(BHT-1)MIM][DEHP] proved that the purity of ionic liquids WAS higher than 95%, which is agreement with the HPLC result.

The TG results of [(BHT-1)MIM][DEHP], presented in Figure 6, indicated that THE decomposition of [(BHT-1)MIM][DEHP] began at approximately 186.1 °C. By 221.9 °C, the weight loss was 5%. The [(BHT-1)MIM][DEHP] was completely decomposed after 371.6 °C. The esterification reaction was conducted at 160 °C, well below the onset temperature, demonstrating the good thermal stability of the bi-functional ionic liquid [(BHT-1)MIM][DEHP] during the reaction. In order to verify this, we performed NMR on the separated ionic liquid after the reaction was completed. The NMR spectra are provided in the Supplementary Material (Figures S5 and S6), and the NMR data are as follows:

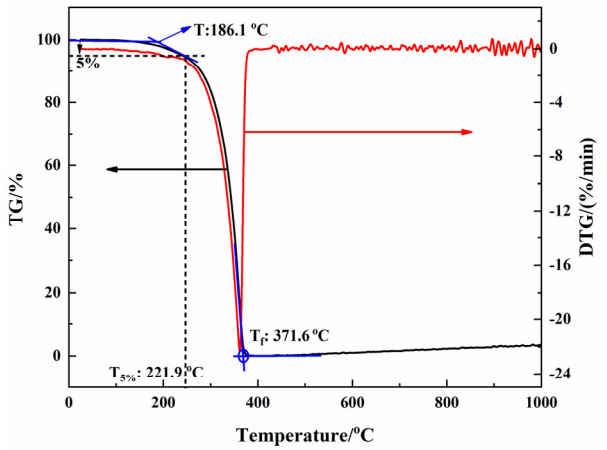


Figure 6. The TG characterization of ionic liquid [(BHT-1)MIM][DEHP].

^{1}H NMR: ($CDCl_3$, 400 MHz, TMS) δ = 10.41 (s, 1H), 7.15 (s, 2H), 7.02 (s, 1H), 6.99 (s, 1H), 5.65–5.30 (m, 3H), 4.05 (s, 3H), 3.78 (d, J = 5.8 Hz, 4H), 1.54–1.47 (m, 2H), 1.42 (s, 18H), 1.38–1.29 (m, 6H), 1.26 (d, J = 4.6 Hz, 10H), 0.82 (t, J = 7.4 Hz, 12H).

^{13}C NMR: ($CDCl_3$, 400 MHz, TMS) δ = 154,74, 138.86, 137.27, 125.97, 123.60, 123.19, 120.78, 67.70, 53.78, 40.37, 34.35, 30.15, 29.00, 23.32, 23.05, 14.06, 10.93.

Figure 7 illustrates the FT-IR spectra, where a peak at 1150 cm^{-1} corresponds to P-O-C and C-O (PETH) stretching vibrations, and another at 1360 cm^{-1} is attributed to P=O stretching [20,21]. The alignment of these peaks in [(BHT-1)MIM][DEHP] with those in PETH + [(BHT-1)MIM][DEHP] confirms the structural stability of [(BHT-1)MIM][DEHP] during the reaction, supporting the conclusions drawn from TG.

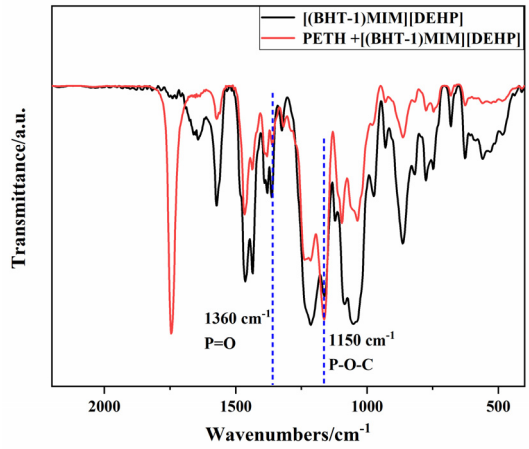


Figure 7. FT–IR spectra of [(BHT-1)MIM][DEHP] and PETH + [(BHT-1)MIM][DEHP].

3.2. Catalytic Performance of [(BHT-1)MIM][DEHP]

The catalytic efficiency of [(BHT-1)MIM][DEHP] was verified by the esterification reaction between pentaerythritol and caproic acid, with results detailed in Table 1. The acid number of products was significantly lower in the presence of catalysts compared to the reaction without catalysts, indicating enhanced catalytic performance. The esterification efficiency was notably improved, achieving 96%, while the yield of pentaerythritol tetra-hexanoate reached 94% under mild reaction conditions. Quantitative ^{1}H NMR is provided in Figure S7, further confirming the high yield and product quality. These results demonstrate the superior catalytic performance of the bi-functional ionic liquid [(BHT-1)MIM][DEHP] in ester oil synthesis. Meanwhile, we also compared the ionic liquid catalyst

with a commercial solid acid catalyst HDN-260, and we found that the esterification was carried out for a longer time compared with the ionic liquid catalyst.

Table 1. The catalytic activity of [(BHT-1)MIM][DEHP].

Entry	Catalyst	Acid Value/(mg KOH/g)	Esterification/%
[a] 1	none	80.61	78
[a] 2	[(BHT-1)MIM][DEHP]	14.37	96 (94) [b]
[c] 3	HDN-260	16.80	95

[a] Reaction conditions: 0.8 g (0.0013 mol) [(BHT-1)MIM][DEHP], 0.013 mol pentaerythritol, 0.052 mol caproic acid, 2 mL toluene, temperature: 160 °C, time: 7 h. [b] The yield of PETH was determined by quantitative ^{1}H NMR with triphenylmethane as internal standard of these products (Figure S7). [c] Reaction conditions: 0.08 g HDN-260, 0.013 mol pentaerythritol, 0.052 mol caproic acid, 2 mL toluene, temperature: 160 °C, time: 23 h.

The structure of the isolated polyol ester was characterized by ^{1}H NMR and ^{13}C NMR in order to provide further evidence on the characterization of the produced polyol ester. The spectra of NMR are provided in the Supplementary (Figures S8 and S9), and the data are provided as follows:

^{1}H NMR($CDCl_3$, 400 MHz, TMS): δ = 4.11 (s, 8H), 2.29–2.32(t, 8H), 1.58–1.63 (m, 8H), 1.26–1.35 (m, 16H), 0.88–0.91 (t, 12H).

^{13}C NMR($CDCl_3$, 400 MHz, TMS): δ = 173.26, 62.13, 41.80, 34.06, 31.24, 24.53, 22.26, 13.86.

3.3. Evaluation of Viscosity, Copper Corrosion, and Oxidation Stability of PETH and PETH + [(BHT-1)MIM][DEHP]

Table 2 presents the kinematic viscosity, viscosity index, and copper strip test results of PETH and PETH + [(BHT-1)MIM][DEHP]. The addition of PETH + [(BHT-1)MIM][DEHP] caused only a slightly increase in viscosity at both 40 °C and 100 °C. During the copper strip tests, no discoloration was observed for either PETH or PETH + [(BHT-1)MIM][DEHP], indicating no reaction with copper. These findings confirm that the bi-functional ionic liquid [(BHT-1)MIM][DEHP] is a suitable additive for PETH. At the same time, we also investigated the oxidative properties of the ionic liquid. PDSC results show that the onset oxidation temperature of PETH containing [(BHT-1)MIM][DEHP] increased from 218 °C to 248 °C, enhancing the antioxidant performance of the base oil. The ionic liquid can act as an antioxidant.

Table 2. The physical and chemical properties of PETH and PETH + [(BHT-1)MIM][DEHP].

Lubricant		PETH	PETH + [(BHT-1)MIM][DEHP]
Kinematic Viscosity /(mm^2/s)	40 °C	18.13	19.56
	100 °C	4.150	4.312
Viscosity index [a]		132	130
Copper strip test/corrosion grade [b]		1a	1a
PDSC oxidation onset temperature [c]/°C		218	248

[a] The viscosity index was measured following the reference [22]. [b] The copper strip test was conducted in accordance with reference [23], under conditions of 100 °C for 3 h, which is designed to assess the relative degree of corrosivity of products. [c] The oxidation onset temperature was determined by the reference [24]: method B.

3.4. Tribological Performance of [(BHT-1)MIM][DEHP]

To evaluate the tribological properties under examination, an Optimol SRV tester was used to measure the friction coefficient of PETH and PETH + [(BHT-1)MIM][DEHP]. Figure 8 depicts the tribological behaviour of PETH and PETH + [(BHT-1)MIM][DEHP]; before 1200 s, the friction coefficient of PETH increases with time, while the friction coefficient of PETH + [(BHT-1)MIM][DEHP] can reach a stable state at 300 s, which indicates

that the addition of ionic liquid not only improves the friction-reducing performance of the base oil but also makes its friction performance more stable. The mean friction coefficient is listed in Table 3; it can be seen that the mean friction coefficient of the base oil PETH is 0.180 (Table 3. entry 1, list 3). Evidently, the friction coefficient (0.110) of PETH plus [(BHT-1)MIM][DEHP] is much lower than the base oil PETH. The bi-functional ionic liquid [(BHT-1)MIM][DEHP] effectively enhances the tribological performance of the base oil PETH. It is possible that a tribofilm is formed through tribo-chemical reactions under high-temperature conditions. [(BHT-1)MIM][DEHP] could achieve a 39% decrease in the friction coefficient, and the anti-wear performance was improved when compared with the ionic liquids with the same anions, namely [C_{11}-IM][DEHP], [N_{888}H][DEHP], [P_{88814}][DEHP], and [N_{12}HHH][DEHP] [18].

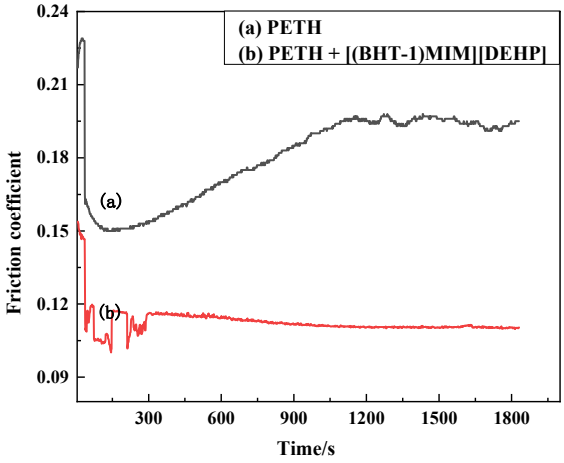


Figure 8. Friction coefficient variation over time for PETH and PETH + [(BHT-1)MIM][DEHP]. (The SRV test was conducted with a load of 50 N, frequency of 25 Hz, temperature of 100 °C, and a stroke length of 1 mm).

Table 3. [a] The mean friction coefficient, the wear scar diameter, and the wear volume of PETH and PETH + [(BHT-1)MIM][DEHP].

Entry	Lubricant	[b] COF Mean	[c] WSD/mm	[d] Wear Volume/10^{-5} mm^3
1	PETH	0.180	0.49	6.69
2	PETH + [(BHT-1)MIM][DEHP]	0.110	0.31	1.24

[a] The SRV test was conducted with a load of 50 N, frequency of 25 Hz, temperature of 100 °C, and stroke length of 1 mm. [b] Average value of the friction coefficient during the test period. [c] The upper running ball. [d] The lower steel disc.

The wear scars of the upper running steel ball lubricated with PETH were analyzed by an OM, as shown in Figure 9a, with a measured wear scar diameter of 0.49 mm. For the steel ball lubricated with PETH + [(BHT-1)MIM][DEHP], the optical image is presented in Figure 9b, showing a significantly reduced wear scar diameter of 0.31 mm, indicating a substantial improvement in anti-wear performance. Quantitative results for the friction coefficient and wear are detailed in Table 3. Furthermore, in the SRV test, the wear volume of the steel disc lubricated with PETH + [(BHT-1)MIM][DEHP] was considerably lower than that of the disc lubricated with PETH alone (Table 2, entries 1 and 2, list 5). Compared with the anti-wear performance of ionic liquids with the same anions at the same time, in ionic liquids [C_{11}-IM][DEHP], [N_{888}H][DEHP], [P_{88814}][DEHP], and [N_{12}HHH][DEHP], the ionic liquid [C_{11}-IM][DEHP] can reduce the wear volume to the minimum, but this is still above 2×10^4 μm^3 [18]. This can be further explained through the presence of

the bi-functional ionic liquid [(BHT-1)MIM][DEHP], which can efficiently improve the anti-wear properties of the base oil PETH.

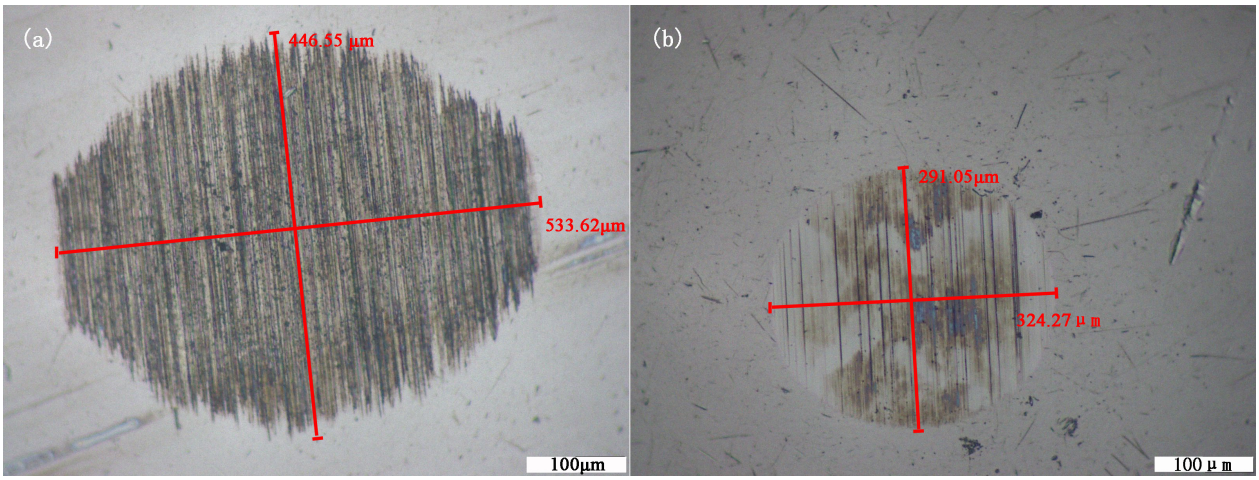


Figure 9. Optical images of the wear scars on the upper running ball lubricated with (**a**) PETH and (**b**) PETH + [(BHT-1)MIM][DEHP]. (The SRV test was conducted with a load of 50 N, frequency of 25 Hz, temperature of 100 °C, and stroke length of 1 mm).

3.5. Analysis of Worn Track

In order to further understand the worn track morphology, FESEM was chosen to characterize the worn surface, as demonstrated in Figure 10. The steel disc lubricated with PETH exhibited significantly wider wear tracks compared to the disc lubricated with PETH plus [(BHT-1)MIM][DEHP]. In contrast, the wear scar of the steel disc lubricated with PETH + [(BHT-1)MIM][DEHP] was narrower and smoother. These observations align with the optical microscope analysis of the steel ball.

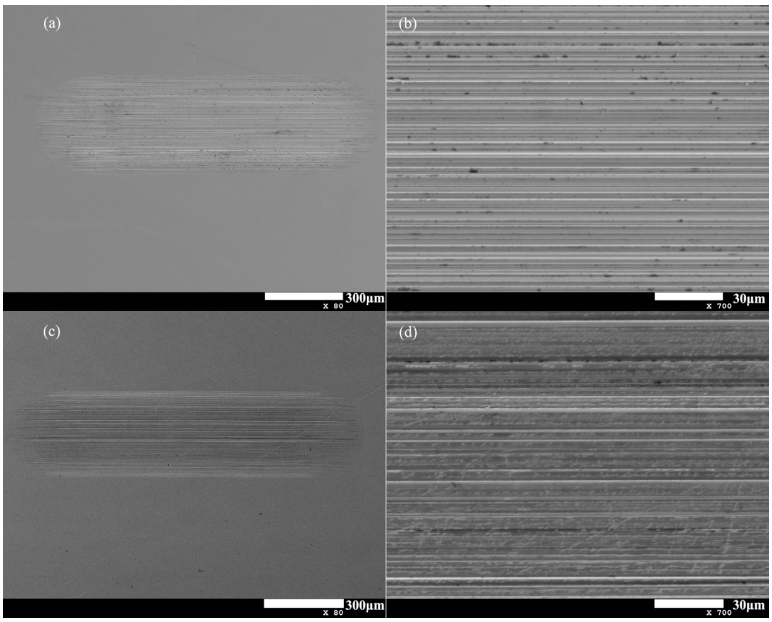


Figure 10. FESEM images showing the worn surfaces of steel discs: (**a**) lubricated with PETH at 80× magnification, (**b**) lubricated with PETH at 700× magnification, (**c**) lubricated with PETH + [(BHT-1)MIM][DEHP] at 80× magnification, and (**d**) lubricated with PETH + [(BHT-1)MIM][DEHP] at 700× magnification. (The SRV test was conducted with a load of 50 N, frequency of 25 Hz, temperature of 100 °C, and a stroke length of 1 mm).

To better inspect the lubrication mechanism of the bi-functional ionic liquid [(BHT-1)MIM][DEHP], the chemical compositions of Fe2*p*, N1*s*, O1*s*, and P2*p* from the worn surface lubricated by PETH + [(BHT-1)MIM][DEHP] were conducted by XPS, and the detailed spectra are shown in Figure 11. It can be seen that the chemical composition of the N1*s*, P2*p*, and O1*s* of the worn surface lubricated by [(BHT-1)MIM][DEHP] changed when compared with the pure [(BHT-1)MIM][DEHP] and the pure PETH. This illustrates that a complicated tribo-chemical reaction happened during the friction process. Peaks of Fe2*p* around 710.8 eV and 724.3 eV are derived from Fe_2O_3, Fe_3O_4, and FeOOH from the worn surface lubricated by PETH + [(BHT-1)MIM][DEHP] [25–27]. The P2*p* signal at 133.70 eV is attributed to $FePO_4$, and around 531.8 eV of O1*s* may belong to $FepPO_4$ and FeOOH [27,28]. The peak of $N1_s$ at 401.04 eV may be attributed to the oxy nitride or nitrogen–nitrogen double bond. The high pressure, heat, catalysis, and mechanical energy generated from the friction test resulted in a tribo-chemical reaction, and Fe_2O_3, Fe_3O_4, FeOOH, and $FePO_4$ were produced, which indicates the boundary lubrication film formed in the contacting zone of PETH + [(BHT-1)MIM][DEHP] during the SRV test; as a result, the friction conduction and anti-wear properties were improved.

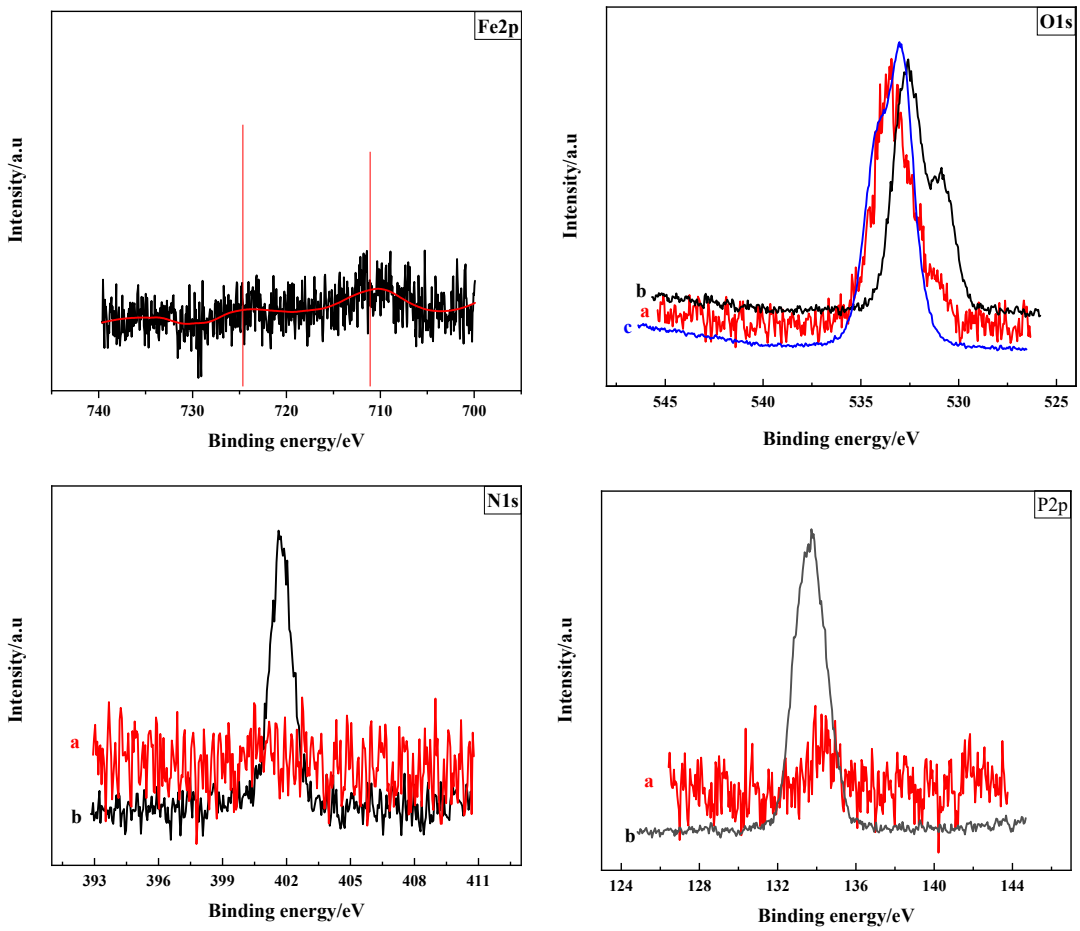


Figure 11. The XPS spectra (**a**) the worn surface lubricated by PETH + [(BHT-1)MIM][DEHP], (**b**) pure [(BHT-1)MIM][DEHP] and (**c**) pure PETH.

4. Conclusions

A bi-functional ionic liquid, 1-(3,5-di-tert-butyl-4-hydroxybenzyl)-3-methylimidazole di(2-ethylhexyl) phosphate ([(BHT-1)MIM][DEHP]), was prepared. The catalytic performance of [(BHT-1)MIM][DEHP] was studied by a model esterification reaction, and the tribological performances of [(BHT-1)MIM][DEHP] were also inspected. Meanwhile, the

lubrication mechanism was investigated. Based on the experimental results, the conclusions are summarized as follows:

(1) The esterification reaction of pentaerythritol with caproic acid was chosen as a model reaction to verify the catalytic performance of the bi-functional ionic liquid [(BHT-1)MIM][DEHP], which acts as a catalyst. The findings indicate that [(BHT-1)MIM][DEHP] exhibits excellent catalytic performance, achieving a high conversion rate of 96% and a 94% yield for the base oil pentaerythritol tetra-hexanoate.

(2) The excellent tribological performances of [(BHT-1)MIM][DEHP], which serves as a lubricant additive, were displayed. The friction coefficient was reduced from 0.180 to 0.110 when compared to the frictional performance of the base oil PETH and PETH plus [(BHT-1)MIM][DEHP] under the same test conditions. This indicates that the friction reduction performance of the base oil PETH was enhanced by the [(BHT-1)MIM][DEHP]. The wear scar diameter and the wear volume of PETH and PETH plus [(BHT-1)MIM][DEHP] decreased from 0.49 mm to 0.31 mm and 6.69×10^{-5} mm^3 to 1.24×10^{-5} mm^3, respectively. It is demonstrated that the anti-wear performance of the base oil PETH was improved efficiently by [(BHT-1)MIM][DEHP].

(3) The bi-functional ionic liquid [(BHT-1)MIM][DEHP] does not need to be separated after the esterification reaction and plays the role of a lubricant additive in ester oil. It not only helps to improve the performance of ester lubricating oil significantly, but also fully enables the synergistic lubrication effect of synthetic ester lubricating oil and ionic liquid.

Supplementary Materials: The following supporting information can be downloaded at https://www.mdpi.com/article/10.3390/lubricants13020045/s1, Figure S1. The HPLC spectra of [(BHT-1)MIM][DEHP]; Figure S2. The schematic diagram of the reaction apparatus; Figure S3. The ^{1}H NMR spectra of [(BHT-1)MIM][DEHP]; Figure S4. The ^{13}C NMR spectra of [(BHT-1)MIM][DEHP]; Figure S5. The ^{1}H NMR spectra of [(BHT-1)MIM][DEHP] (after the esterification); Figure S6. The ^{13}C NMR spectra of [(BHT-1)MIM][DEHP] (after the esterification); Figure S7. The ^{1}H NMR spectra of PETH+ [(BHT-1)MIM][DEHP]; Figure S8. The ^{1}H NMR spectra of PETH; Figure S9. The ^{13}C NMR spectra of PETH; Table S1. The vendors and quality or grade of chemicals; Table S2. The element analysis of [(BHT-1)MIM][DEHP] and PETH + [(BHT-1)MIM][DEHP] before friction test.

Author Contributions: Experimental designing, data collection and analysis, writing manuscript, Y.W.; supervision, H.S.; formal analysis, J.Y.; investigation, C.J. and Q.Z.; editing, W.L.; conceptualization, Q.J. All authors have read and agreed to the published version of the manuscript.

Funding: This research was funded by the National Natural Science Foundation of China, grant number 52105226, Taishan Scholar Youth Expert Program, and Gansu Province Intellectual Property Plan, grant number 22ZSCQD03.

Data Availability Statement: Data will be made available on reasonable request.

Conflicts of Interest: The authors declare no conflicts of interest.

References

1. Patil, S.; Rajurkar, K.; Patil, S.; Pratap, A. Synthesis of guerbet esters and its application in drilling and grinding oil. *Tribol. Int.* **2023**, *177*, 107993. [CrossRef]
2. Salimon, J.; Salih., N. Epoxidized malaysian elaeis guineensis palm kernel oil trimethylolpropane polyol ester as green renewable biolubricants. *Biomass Bioenergy* **2023**, *175*, 106883. [CrossRef]
3. Hamdan, S.H.; Chong, W.W.F.; Ng, J.H.; Chong, C.T.; Zhang, H. Nano-tribological characterization of palm oil-based trimethylolpropane ester for applicaiton as boundary lubricant. *Tribol. Int.* **2018**, *127*, 1–9. [CrossRef]
4. Nifant'ev, I.; Bagrov, V.; Vinogradov, A.; Vinogradov, A.; Ilyin, S.; Sevostyanova, N.; Batashev, S.; Ivchenko, P. Methylenealkane-based low-viscosity ester oils: Synthesis and outlook. *Lubricants* **2020**, *8*, 50. [CrossRef]

5. Wang, Y.Q.; Liang, Y.X.; Li, Y.Y.; Rui, W.Q.; He, J.J.; Zhao, M.Y. Synthesis, tribological properties and oxidative stability of polyol esters base oils containing pentaerythritol complex esters. *Tribol. Int.* **2024**, *195*, 109618. [CrossRef]
6. Ma, X.; Liu, F.; Helian, Y.; Li, C.; Wu, Z.; Li, H.; Chu, H.; Wang, Y.; Wang, Y.; Lu, W.; et al. Current application of MOFs based heterogeneous catalysts in catalyzing transesterification/esterification for biodiesel production: A review. *Energy Convers. Manag.* **2021**, *229*, 113760. [CrossRef]
7. Feuge, R.O.; White, J.L.; Brown, M. Preparation of fatty acid esters of polyol glucosides. *J. Am. Oil Chem. Soc.* **1978**, *55*, 699–702. [CrossRef]
8. Zhang, F.X.; Zhang, G.X. Microwave-promoted synthesis of polyol esters for lubrication oil using a composite catalyst in a solvent-free procedure. *Green Chem.* **2011**, *13*, 178–184. [CrossRef]
9. Varhadi, P.; Kotwal, M.; Srinivas, D. Zirconium phenyl phosphate phosphite as a highly active, reusable, solid acid catalyst for producing fatty acid polyol esters. *Appl. Catal. A Gen.* **2013**, *462–463*, 129–136. [CrossRef]
10. Singh, R.K.; Gupta, P.; Sharma, O.P.; Ray, S.S. Homogeneous synthesis of cellulose fatty esters in ionic liquid (1-butyl-3-methylimidazolium chloride) and study of their comparative antifriction property. *J. Ind. Eng. Chem.* **2015**, *24*, 14–19. [CrossRef]
11. Ma, X.T.; Zhang, Y.; Song, Z.J.; Yu, K.; He, C.L.; Zhang, X. Enzyme-catalyzed synthesis and properties of polyol ester biolubricant produced from rhodotorula glutinis lipid. *Biochem. Eng. J.* **2021**, *173*, 108101. [CrossRef]
12. Ruzamil, R.N.M.; Yusup, S.; Rashid, U. Optimization of polyol ester production by transesterification of jatropha-based methyl ester with trimethylolpropane using taguchi design of experiment. *Fuel* **2011**, *90*, 2343–2345.
13. Gupta, R.; Yadav, M.; Gaur, R.; Arora, G.; Sharma, R.K. A straightforward one-pot synthesis of bioactive N-aryl oxazolidin-2-ones via a highly efficient Fe_3O_4@SiO_2-supported acetate-based butylimidazolium ionic liquid nanocatalyst. *Green Chem.* **2017**, *19*, 3801–3812. [CrossRef]
14. Zeng, Y.; Chen, H.; Hu, G.; Cai, R.; Chengyang, Y.; Huang, Z.; Han, B. Novel proline trifluoromethanesulfonate ionic liquid as an effective and renewable catalyst for oleic acid esterification: Process optimization, kinetic studies, and thermodynamic studies. *Ind. Crops Prod.* **2024**, *216*, 118778. [CrossRef]
15. Cai, R.; Hu, G.; Chenyang, Y.; Huang, Z.; Wang, X.; Han, B. Amino-acid-functionalized methanesulfonate ionic liquids as effective and reusable catalysts for oleic acid esterification. *Sustain. Mater. Technol.* **2025**, *43*, e01190. [CrossRef]
16. Roy, S.; Speed, L., Jr.; Viola, M.; Luo, H.; Leonard, D.; Qu, J. Oil miscible phosphonium-phosphate ionic liquid as novel antiwear and antipitting additive for low-viscosity rear axle lubricants. *Wear* **2021**, *466–467*, 203588. [CrossRef]
17. Bai, Z.; Qiu, J.; Zhang, D.; Gao, P.; Jian, Z. Tribological behavior of 1, 8-diazabicyclo[5.4.0] undecane-7-ene-organophosphoric acid-based protic ionic liquids as lubricant additives. *Tribol. Lett.* **2023**, *71*, 105. [CrossRef]
18. Fang, H.; Li, Y.; Li, H.; Zhang, S.; Ding, Q.i.; Yu, W.; Hu, L. Tribological behavior at electronic scales for an oil-soluble ionic liquid with extremely low effective addition and highly load bearing capacity. *Chem. Eng. J.* **2023**, *465*, 142810. [CrossRef]
19. *ISO 6618: 1997 (E)*; Petroleum Products and Lubricants-Determination of Acid or Base Number-Colour-Indicator Titration Method. International Organization for Standardization: Geneva, Switzerland, 1997.
20. Liu, Q.; He, H.a.o.; Chao, Z.; Xie, J.; Ruchenstein, E. Synthesis of mesoporous chromium phosphates via solid-state reaction at low temperature. *New J. Chem.* **2012**, *36*, 139–147.
21. Wolak, A.; Krasodomski, W.; Zajac, G. FTIR analysis and monitoring of used synthetic oils operated under similar driving conditions. *Friction* **2020**, *8*, 995–1006. [CrossRef]
22. *ASTM D2270-24*; Standard Practise for Calculating Viscosity Index from Kinematic Viscosity at 40 °C and 100 °C1,2. ASTM International: West Conshohocken, PA, USA, 2024.
23. *ASTM D130-10*; Standard Test Method for Corrosiveness to Copper from Petroleum Products by Copper Strip Test. ASTM International: West Conshohocken, PA, USA, 2010.
24. *ASTM E2009-23*; Standard Test Methods for Oxidation Onset Temperature of Hydrocarbons by Differential Scanning Calorimetry. ASTM International: West Conshohocken, PA, USA, 2023.
25. Han, Y.Y.; Qiao, D.; Guo, Y.X.; Feng, D.P.; Shi, L. Influence of competitive adsorption on lubricating property of phosphonate ionic liquid additives in PEG. *Tribol. Lett.* **2016**, *64*, 22. [CrossRef]
26. Grace, J.; Vysochanska, S.; Lodge, J.; Iglesias, P. Ionic liquids as additives of coffee bean oil in steel-steel contacts. *Lubricants* **2015**, *3*, 637–649. [CrossRef]
27. Guo, H.; Stoyanovich, B.; Pang, J.; Iglesias, P. Lubricating ability of proic ionic liquid as additives to a biodegradable oil for aluminum-steel contact: Effect of alkyl chain length and propensity to hydrogen bonding. *Lubricants* **2023**, *11*, 329. [CrossRef]
28. Zu, P.J.; Zhang, Y.S.; Zhang, S.W.; Li, Y.; Hu, L.T. Excellent corrosion inhibition and lubrication performance of MMT based ionic liquids as ester oil additives. *Tribol. Int.* **2024**, *194*, 109473. [CrossRef]

Disclaimer/Publisher's Note: The statements, opinions and data contained in all publications are solely those of the individual author(s) and contributor(s) and not of MDPI and/or the editor(s). MDPI and/or the editor(s) disclaim responsibility for any injury to people or property resulting from any ideas, methods, instructions or products referred to in the content.